Band-gap creation by icosahedral symmetry in nearly-free-electron materials

A. E. Carlsson
Department of Physics, Washington University, Campus Box 1105, One Brookings Drive, St. Louis, Missouri 63130
(Received 22 September 1992)

A series of numerical electronic density-of-states calculations is performed for rational approximants to a model one-electron potential based on icosahedrally arranged plane-wave components. It is found that high-order approximants can have band gaps even if the low-order approximants do not; furthermore, the magnitude of the gap increases with the order of the approximant. The results are interpreted via a two- and three-wave analysis of the energy eigenvalues at the pseudo-Jones-zone faces and edges. It is also found that the mechanism of band-gap reduction in the rational approximants is the presence of a small density of gap states. An analytic calculation shows that these gap states result from a splitting of threefold and pseudothreefold states at the valence-band edge when the icosahedral symmetry is broken. The splitting is proportional to the error with which the ratio between the approximant indices approximates τ, the golden mean. Finally, an application to the AlCuLi system is presented.

I. INTRODUCTION

This paper addresses the mechanisms by which icosahedral symmetry, by itself, increases the tendency toward gap of quasigap formation in nearly-free-electron (NFE) -type quasicrystals. This effort is motivated by (1) recent conductivity,[1,2] specific-heat,[1-4] and photoemission[5,6] experiments, which have suggested a strongly reduced Fermi-level density of states (DOS) in some stable NFE quasicrystals and their rational approximants, and (2) quantitative electronic-structure calculations[7] for stable rational approximants, which have found pronounced dips in the electronic DOS, or quasigaps, around the Fermi level. The mechanism of quasigap formation in icosahedral quasicrystals has previously been addressed[8-11] using essentially a two-plane-wave analysis based on the "pseudo-Jones zone." This is the polyhedron in reciprocal space defined by the planes bisecting the dominant **Q** vectors in the one-electron potential. In a crystal, if these **Q** vectors are the smallest reciprocal-lattice vectors, then the pseudo-Jones zone becomes equivalent to the first Brillouin zone. Couplings between opposing faces of the pseudo-Jones zone lead to gaps at particular **k** vectors, which become valleys and peaks in the DOS upon **k**-space integration and can lead to gaps in the DOS if the potential is strong enough. The Fermi-level DOS is most strongly perturbed if **Q** is close to $2k_f$. The earlier analysis has shown that the icosahedral arrangement has enhanced quasigap effects because of the high degeneracy of some shells of reciprocal-lattice vectors.

The present analysis focuses on a complementary effect, namely the effect of the *arrangement* of the quasi-reciprocal-lattice vectors in a shell whose *number of quasi-reciprocal-lattice vectors is fixed at twelve.* I first perform numerical calculations for periodic rational-approximant structures. These utilize a finite-dimensional secular determinant obtained by using a plane-wave basis with a kinetic-energy cutoff. I find that a small unit-cell cubic crystal can never have a gap, but sufficiently high-order rational approximants can have a gap if the potential is strong enough. Subsequently, I present two analytic calculations. The first is based on the pseudo-Jones-zone analysis and extends the earlier analysis to the edges and corners of the Jones zone, which have been treated[12] for periodic crystals but have not, to my knowledge, been analyzed for icosahedral phases. The second analytic calculation treats gap states that are seen in the numerical results. At Bloch wave-vector zero, the symmetry is high enough that some parts of the secular matrix can be diagonalized analytically. It is found that the gap states correspond to particular combinations of threefold and pseudothreefold wave vectors and that their penetration into the gap is due to a splitting of the valence-band edge caused by the lowered symmetry relative to the icosahedral case. Finally, I argue that some of the effects seen in the calculations may be relevant to the AlCuLi system.

II. MODEL POTENTIAL AND METHOD

The one-electron potential is modeled as follows:

$$V(r)=V_0\sum_{i=1}^{12}\exp(i\mathbf{Q}\cdot\mathbf{r})\ , \tag{1}$$

where all of the twelve **Q** vectors have the same magnitude Q_0. I take $V_0>0$. For the metals typically found in NFE quasicrystals, the atomic pseudopotential $V_{ps}(Q)$, is, in fact, positive[13] at $Q=2k_f$. This potential is clearly highly idealized but exhibits in the simplest fashion the effects of interest here.

The case of greatest interest is that in which the **Q** vectors in Eq. (1) are arranged icosahedrally. Unfortunately, existing numerical methods cannot treat this case, since the **Q** vectors are incommensurate, and there is thus no translational periodicity. However, one can approximate the icosahedral arrangement arbitrarily closely by a set of commensurate **Q** vectors:

$$\mathbf{Q}_i=[Q_0/(m^2+n^2)^{1/2}](\pm n,\pm m,0)$$

and cyclic permutations of this form. The icosahedral arrangement corresponds to $n/m=\tau=1(1+\sqrt{5})/2=1.618\ldots$. I use the Fibonacci sequence of approximations to τ: $\{1/1,2/1,3/2,5/3,\ldots\}$. In order to prevent a possible misunderstanding, I point out that the notation $n/m=1/1$ does not correspond to the usual "1/1" rational approximant defined by the orientation of a hyperplane in six-dimensional space; the latter corresponds to $n/m=5/3$. Similarly, the usual "2/1" rational approximant corresponds to $n/m=8/5$.

In general, the rational-approximant potential is invariant under translations of

$$a=2\pi(n^2+m^2)^{1/2}/Q_0 , \tag{2}$$

in the x, y, and z directions. Thus one has, at the worst, a simple-cubic Bravais lattice with lattice constant a. Provided one takes a finite kinetic-energy cutoff, it is possible to set up a secular matrix of finite dimension, which can be numerically diagonalized. If n and m are both odd, then an additional symmetry is present, and the Bravais lattice is bcc; for $n=m=1$, one simply has the familiar fcc shell of twelve reciprocal-lattice vectors, which comes from the bcc Bravais lattice. We choose $(\hbar^2/2m)Q_0^2=3.2$ Ry, which in the simplest Jones-zone analysis give a face-center gap centered at $(\hbar^2/2m)(Q_0/2)^2=0.8$ Ry; this is roughly comparable to the energies at which quasigaps are found in the *ab initio* calculations.[7] We use a kinetic-energy cutoff of 2.0 Ry, which is more than twice as high as the energy of the quasigap. This allows us to go as high as $n/m=8/5$ in the rational approximants. My calculations using higher cutoffs up to 5 Ry for lower-order approximants show the same trends as the 2.0-Ry results. To avoid having discontinuities in band energies, which would result from an abrupt cutoff, we use a smooth energy-dependent cutoff giving Hamiltonian matrix elements of the form

$$\langle\mathbf{k}+\mathbf{Q}|V|\mathbf{k}\rangle=[f(|\mathbf{k}+\mathbf{Q}|)f(k)/f(Q_0/2)^2]V_0 , \tag{3}$$

where

$$f(k)=\exp\{-\alpha E_{\max}/[E_{\max}-E(k)]\} ,$$

$E_{\max}$ is the energy cutoff, $E(q)$ is the free-electron energy of $\mathbf{q}$, and α is arbitrarily chosen to be 0.05. With this form for the matrix elements, $\langle\mathbf{k}+\mathbf{Q}|V|\mathbf{k}\rangle=V_0$ if $|\mathbf{k}+\mathbf{Q}|=k=Q_0/2$.

III. NUMERICAL DENSITY-OF-STATES RESULTS

Results for $V_0=0.25$ Ry, are shown in Fig. 1(a). The $n/m=1/1$ results, corresponding to a simple bcc crystal, have a fairly deep minimum corresponding to a quasigap. The overall behavior is fairly similar to *ab initio* results[14] for bcc Li. I find that no matter how strong the potential is (as long as V_0 is positive), the 1/1 arrangement produces no gap in the DOS. As one goes to the higher approximants, the minimum value of the DOS drops to a very low value in the 3/2 case. Beginning with the 5/3 results, a gap develops. Thus it is possible for a nearly icosahedral structure to have a gap in circumstances in which a smaller-unit-cell cubic structure does not. The magnitude of the gap increases as n/m goes to 8/5. Figure 1(b) shows similar results for $V_0=0.13$ Ry. In this case, the potential is not strong enough to produce a gap even for the 8/5 case, but a minimum or quasigap in the DOS is present. The trend toward increasing gapping effects with the higher-order approximants is seen again;

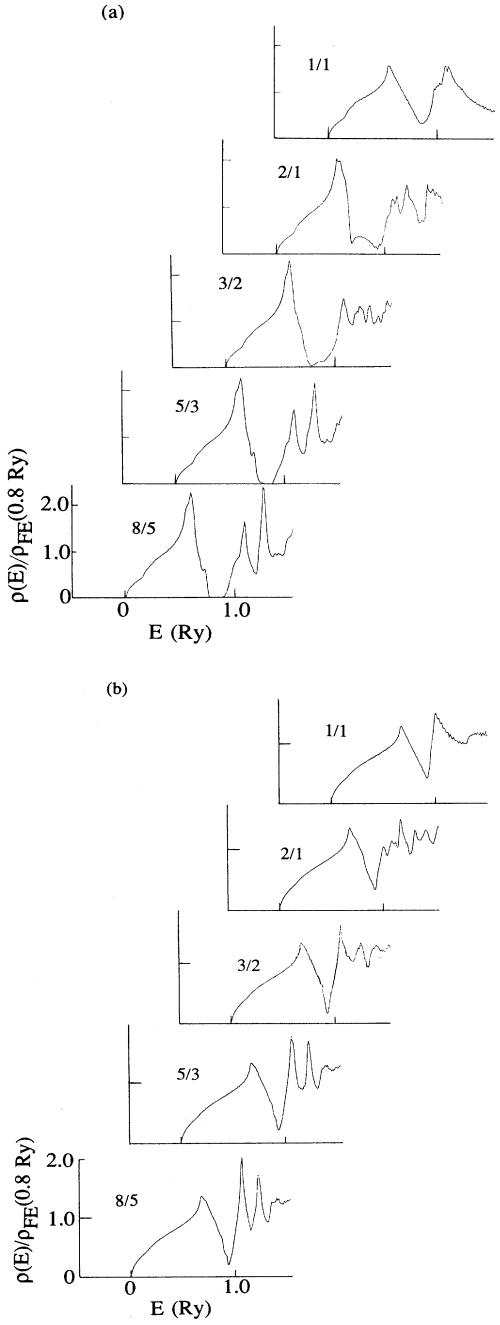

FIG. 1. (a) Calculated DOS distributions $\rho(E)$ for rational-approximant structures, for $V_0=0.25$ Ry. DOS given in units of the free-electron DOS at $E=0.8$ Ry. (b) Calculated DOS distributions for rational-approximant structures, for $V_0=0.13$ Ry.

the minimum value of the DOS for the 8/5 case is roughly half of that for the 1/1 case. However, unlike the $V_0=0.25$ Ry case, the behavior around the gap region is essentially converged already for the $n/m=3/2$. The electronic structure is expected to converge more rapidly with the order of the rational approximant for weaker potentials. To second order in V_0, for example, only the magnitudes of the **Q** vectors and the value of V_0 enter the DOS; the angles between the **Q** vectors enter only in higher orders of perturbation theory. The magnitudes of the **Q** vectors are the same for all of the approximants. Thus, if the potential were sufficiently weak for a second-order treatment to be accurate, then all of the approximants would have essentially the same DOS.

IV. PSEUDO-JONES-ZONE ANALYSIS

I now give a simplified physical interpretation of the above numerical results in terms of the energy eigenvalues on the faces of the pseudo-Jones zone. The familiar twelve-sided first Brillouin zone for the 1/1 case is shown in Fig. 2(a). For the **k** vectors N at the centers of the faces, $\mathbf{k}=(\pm\pi/a,\pm\pi/a,0)$, most of the physics is given by a two-plane-wave analysis involving **k** and $-\mathbf{k}$. This gives the energy eigenvalues $E(k)=(\hbar^2/2m)(2\pi^2/a^2)\pm V_0$, resulting in a gap of magnitude $2V_0$. (Here I ignore the effects of the energy-dependent cutoff). The lower edge of the gap is thus nondegenerate. Consider now the edge-center point $F=(2/3)(2\pi/a,\pi/a,\pi/a)$. This point is coupled to two other equivalent **k** points of type F (one of which is indicated in the figure) by the $\mathbf{Q}=(-2\pi/a,-2\pi/a,0)$ and $(-2\pi/a,0,-2\pi/a)$ potential components; these two **k** points are in turn coupled to each other by the $\mathbf{Q}=\pm(0,2\pi/a,-2\pi/a)$ components. Thus there is a threefold degenerate subspace, and one has to use a three-wave analysis. The Hamiltonian matrix for the three plane waves has the form

$$\begin{pmatrix} E_0 & V_0 & V_0 \\ V_0 & E_0 & V_0 \\ V_0 & V_0 & E_0 \end{pmatrix},$$

where E_0 is the kinetic energy at F. The eigenvalues are then E_0+2V_0, and E_0-V_0, with the latter being doubly degenerate. For $V_0>0$, the latter is the lowest-energy state.

Consider the line connecting F to N. Of the two bands emerging from the lower, doubly degenerate state at F, the three-plane-wave analysis indicates that one connects to the top of the gap at N and one to the bottom, as shown in Fig. 3(a). Thus the gap at N is "erased" by effects at the edge of the Jones zone. Even if the band hookup is not the same as indicated by the three-plane-wave model, or the energy at F is not inside the N-point gap, one can readily show that it is topologically impossible to connect the eigenvalues at N to those at F without erasing the gap at N. This result is based only on the degeneracy of the lowest state at F. Therefore, it is likely valid when additional components are "turned on" as well, provided they are not strong enough to change the ordering of the eigenvalues at F.

Consider now the icosahedral pseudo-Jones zone, shown in Fig. 2(b). The twelve **Q** vectors have the form $\mathbf{Q}=Q_0/(1+\tau^2)^{1/2}(\pm,\tau,\pm1,0)$, along with cyclic permutations. As in the cubic case, the eigenvalues at the face centers are given by $E=(\hbar^2/2m)(Q_0^2/4)\pm V_0$, and the gap has magnitude $2V_0$. The edge center $F=Q_0/(1+\tau^2)^{1/2}(\sqrt{5}/2,0,0)$ is connected by the $(-\tau,\pm1,0)$-type potential components to two other **k** vectors $\mathbf{k}=Q_0/(1+\tau^2)^{1/2}(-\frac{1}{2},\pm1,0)$ having the same length as F. However, in contrast to the fcc arrangement, these **k** vectors are not equivalent to F. In addition, they are not connected by any of the **Q**'s contributing to the potential. Thus the matrix for the threefold-degenerate subspace has the form

$$\begin{pmatrix} V_0' & V_0 & 0 \\ V_0 & E_0' & V_0 \\ 0 & V_0 & E_0' \end{pmatrix},$$

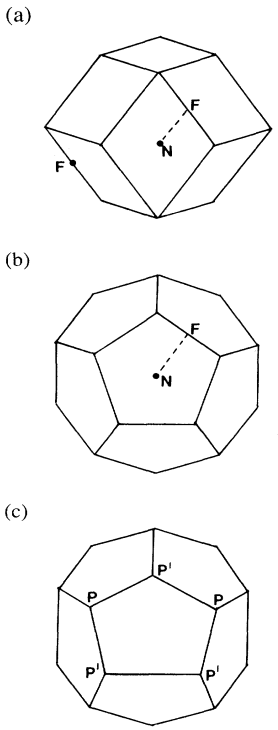

FIG. 2. Jones and pseudo-Jones zones for (a) $n/m=1/1$, (b) $n/m=\tau$, and (c) $n/m=2/1$.

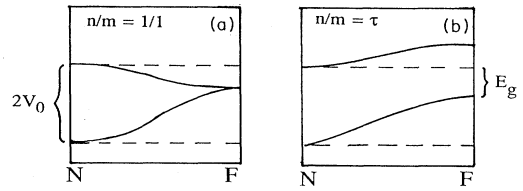

FIG. 3. Likely band lineups for (a) cubic $n/m=1/1$ and (b) $n/m=\tau$. In (b), E_g indicates band gap.

where E_0' is the kinetic energy associated with the point F. The eigenvalues of this matrix are *nondegenerate:* E_0' and $E_0' \pm \sqrt{2} V_0$. Thus, the band connections shown in Fig. 3(b) are plausible; unlike the cubic case, it is possible to have a band gap in the DOS. A parallel four-wave analysis for the corners of the Jones zone also yields a nondegenerate lowest eigenvalue, and allows the possibility of a band gap.

I now show that if the **Q** vectors are rational approximants to the icosahedral ones, then the magnitude of the band gap, if one exists, increases with the order of the rational approximant as icosahedral symmetry is approached. This result is expected on the basis of the near-sphericity of the pseudo-Jones zone. It is independent of the sign of V_0. Since the threefold corners of the icosahedral pseudo-Jones zone have the highest kinetic energy, one would expect the valence-band edge states to be built out of the corresponding plane waves. In the rational-approximant Jones zones, illustrated in Fig. 1(c) for the 2/1 case, these 20 corners split into two classes. One class contains eight corners P in (111)-type directions. The other has twelve members P', in $(n,m,0)$-type directions. Of these two classes, one has higher free-electron energy than in the icosahedal case and one has lower free-electron energy, leading to a splitting of the valence-band edge. The choice of which class is higher depends on whether n/m is greater or less than τ. The 30 edge centers similarly split into two classes. In fact, any crystallographically related collection of points on the boundary of the icosahedral pseudo-Jones zone having more than twelve members is split in the rational approximants. The only collection of points having twelve or fewer members is the face centers. Thus, if either the valence- or conduction-band edge occurs away from the face centers, this edge is split in the rational approximant. The band gap is then reduced. The analytic results to be presented in the next section confirm this band-edge splitting mechanism for the reduction of the band gap.

V. GAP STATES

A remarkable feature of the numerical results obtained here is that the reduction of the band gap in the rational approximants relative to the icosahedral case occurs via the appearance of a small density of gap states, rather than through overall shifts in the band edges. This is shown in detail in Fig. 4, which magnifies the band-gap region of the "5/3" plot in Fig. 1(a). While the conduction-band edge is quite sharp, a low density of gap states is seen between roughly $E=0.76$ and 0.82 Ry. I find that the width of the gap states drops with increasing order of the rational approximant; also as the order increases, the placement of the gap states alternates between the valence-band and conduction-band edges.

The origin of the gap states can be seen via an analytic calculation of the eigenvalues at $\mathbf{k}=\mathbf{0}$ around the valence-band edge in the 5/3 case; we shall see that this calculation confirms the simplified pseudo-Jones zone analysis presented above. Note that **k** denotes the Bloch wave vector corresponding to the cubic lattice constant,

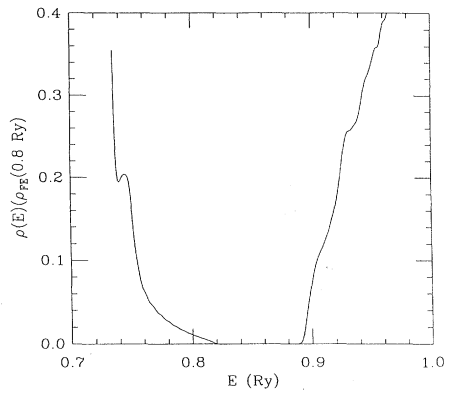

FIG. 4. Expanded picture of electronic DOS in the region of the band gap, for $V_0=0.25$ Ry and $n/m=5/3$.

not the physical momentum entering the pseudo-Jones zone analysis. Analysis of the numerical wave functions shows that the upper edge of the gap states is, in fact, at $\mathbf{k}=\mathbf{0}$. At this value of **k**, the wave functions are built up entirely of reciprocal-lattice vectors **K**. The calculated wave functions also show that the states around the valence-band edge are dominated by the following **K** vectors, in units of $2\pi/a$: (3,0,1), (2,2,2), (3,1,2), and (4,0,0). The potential does not have the full 48-fold symmetry of the cubic lattice because the potential matrix element for the momentum transfer $\mathbf{Q}=(5,3,0)$ (V_0) does not equal that for $\mathbf{Q}=(3,5,0)$ (0). All cyclic permutations and sign changes are included in the symmetry operations of the potential, but permutations that exchange only two indices are not. Thus for example, (3,0,1) is equivalent to $(1,-3,0)$, but not to (1,0,3). Therefore, it is important to keep in mind the ordering of the spatial coordinates in the (3,0,1)- and (3,1,2)-type components of the wave function.

The free-electron energies of these **K** vectors, obtained via Eq. (2), are given in Table I, along with the values of $f(K)/f(Q_0/2)$ that enter the potential matrix elements in Eq. (3). The nonzero couplings are between pairs of the following types, along with those obtained from these by the symmetry operations given above. (Note that each symmetry operation has to be applied simultaneously to both of the vectors that are coupled.)

$$\begin{aligned}&(3,0,1)\Longleftrightarrow(-2,3,1)(2,-3,1),(0,0,-4)\\&(2,2,2)\Longleftrightarrow(2,-3,-1),(-1,2,-3)(-3,-1,2)\ .\end{aligned}\tag{4}$$

TABLE I. Free-electron energies and f factors [cf. Eq (3)] for $n/m=5/3$ and $n/m=\tau/1$.

	K	$E_0(\mathbf{K})$ (Ry)	$f(K)/f(Q_0/2)$
5/3	(3,0,1)	0.941	0.989
	(2,2,2)	1.129	0.969
	(3,1,2)	1.318	0.939
	(4,0,0)	1.505	0.890
$\tau/1$	$(\tau-1,\tau-1,\tau-1)$	1.013	0.982
	$(2(\tau-1),0,0)$	1.351	0.932

Thus the first two shells in Table I couple only to the second two and vice versa. All intrashell couplings vanish. Although the (2,2,2)- and (3,0,1)-type **K** vectors are not directly coupled, they do have an indirect coupling via the (3,1,2) shell. For example (3,0,1) is coupled directly to $(-2,\pm 3,1)$, which is in turn coupled to $(-2,\pm 2,-2)$. Thus the indirect coupling of (3,0,1) to $(-2,2,-2)$ equals its indirect coupling to $(-2,-2,-2)$. However, it is possible to construct a wave function that has nonzero components in the (2,2,2) shell, but vanishing components in the (3,0,1) shell. To see this, consider a wave function of the form

$$|\psi_{222}\rangle=(1/\sqrt{8})[|2,2,2\rangle-|-2,2,2,\rangle-|2,-2,2,\rangle-|2,2,-2\rangle$$
$$+|2,-2,-2\rangle+|-2,2,-2\rangle+|-2,-2,2\rangle-|-2,-2,-2\rangle] .$$

Because $|-2,2-2\rangle$ and $|-2,-2,-2\rangle$ appear with opposite signs in $|\psi_{222}\rangle$, the indirect coupling between $|3,0,1\rangle$ and $|\psi_{222}\rangle$ vanishes; the same is, of course, true for all of the other members of the (3,0,1) shell by symmetry considerations. Thus, one can construct a wave function containing only $|\psi_{222}\rangle$ and (3,1,2)-type **K** vectors. The linear combination of (3,1,2)-type **K** vectors that couples to $|\psi_{222}\rangle$ has the form

$$|\psi_{312}\rangle=(1/\sqrt{24})[\{|2,-3,-1\rangle+|-1,2,-3\rangle+|-3,-1,2\rangle\}-\{|-2,-3,-1\rangle+|1,2,-3\rangle+|3,-1,2\rangle\}-\cdots] ,$$

where each group of three **K** vectors in curly braces couples to one member of the (2,2,2) shell, according to Eq. (4). The signs in front of these groups are the same as those in $|\psi_{222}\rangle$. One then finds that $\langle\psi_{222}|H|\psi_{312}\rangle=\sqrt{3}\tilde{V}_0$, where $\tilde{V}_0$ includes the effects of the f factors in Eq. (3). Thus the possible eigenvalues associated with this type of wave function are given by the eigenvalues of the following matrix:

$$\begin{bmatrix} E_0(222) & \sqrt{3}\tilde{V}_0 \\ \sqrt{3}\tilde{V}_0 & E_0(312) \end{bmatrix} ,$$

which are

$$\bar{E}\pm\sqrt{\Delta E^2+3\tilde{V}_0^2} , \tag{5}$$

where $\bar{E}=[E_0(222)+E_0(312)]/2$ is the average of the kinetic energies of the (2,2,2) shell and the (3,1,2) shells, and

$$\Delta E=[E_0(222)-E_0(312)]/2$$

is their difference. The eigenvalue corresponding to the minus sign in Eq. (5) is 0.818 Ry, in very close agreement with the edge of the gap states seen in Fig. 4. My analysis of the numerically obtained wave functions confirms that this is the correct wave function. We note that the (2,2,2) directions have true threefold symmetry. One readily sees that the wave function itself also has true threefold symmetry, in the sense that rotation about any of the threefold axes leaves the wave function invariant. I note that the identification of the wave functions around the valence-band edge with the threefold axes is consistent with the pseudo-Jones-zone analysis performed above.

One can similarly build states out of the (3,0,1) shell that do not couple to the (2,2,2) shell. As we shall see later, the (3,0,1) shell is pseudothreefold, in that as the order of the rational approximant increases, the (3,0,1) **K** vectors gradually become equivalent to the (2,2,2) vectors. In this case, the wave function is built out of the (3,0,1) shell, the (3,1,2) shell, and the (4,0,0) shell. We first ignore the (4,0,0) shell and treat exactly the remaining part of the Hamiltonian. Then the analysis is entirely parallel to the preceding case, except that each member of the (3,0,1) shell couples only to two members of the (3,1,2) shell. This leads to a matrix element $\langle\psi_{301}|H|\psi_{312}\rangle=\sqrt{2}\tilde{V}_0$, rather than the $\sqrt{3}$ factor obtained before. Here, $|\psi_{301}\rangle$ is any linear combination of K vectors in the (3,0,1) shell, which is not indirectly coupled to the (2,2,2) shell; since the (3,0,1) shell has twelve members and the (2,2,2) shell has eight members, the noncoupling condition corresponds to a system of eight equations in twelve unknowns, which must have at least four solutions. $|\psi_{312}\rangle$ is the corresponding linear combination of **K** vectors in the (3,1,2) shell, according to Eq. (4). The factor of 3 in Eq. (5) is then replaced by a factor of 2, and one obtains an energy of 0.751 Ry. Inclusion of the (4,0,0) shell by second-order perturbation theory leads to a downwards of approximately 0.025 Ry, and thus a final energy of 0.726 Ry. This eigenvalue is fourfold degenerate because of the multiplicity of solutions for $|\psi_{301}\rangle$; this is again confirmed by the numerical results.

The difference between the energies of the threefold and pseudothreefold states calculated here is a measure of the strength of the deviation from icosahedral symmetry. To see this, we generalize the above analysis to arbitrary n/m. The **K**-vector shells are then as follows:

$$(3,0,1)\Longrightarrow(m,0,2m-n) ,$$
$$(2,2,2)\Longrightarrow(n-m,n-m,n-m) ,$$
$$(3,1,2)\Longrightarrow(m,2m-n,n-m) ,$$
$$(4,0,0)\Longrightarrow(2(n-m),0,0) .$$

In the limit of icosahedral symmetry, $n/m\rightarrow\tau/1$, the radii of the first two shells become the same, since

$$3(n-m)^2-[m^2+(2m-n)^2]\rightarrow 2(\tau^2-\tau-1) ,$$

which vanishes for $\tau=(1+\sqrt{5})/2$. Thus the twelve (3,0,1) and eight (2,2,2) K vectors merge into a single shell of 20 threefold vectors, which correspond to the corners of an icosahedron. It is thus legitimate to call the (3,0,1) vectors pseudothreefold. Similarly, the 24 (3,1,2) and six

(4,0,0) **K** vectors merge into a shell of 30 twofold vectors, which correspond to the edge centers of an icosahedron.

In the limit of icosahedral symmetry, the valence-band-edge energy can readily calculated. The kinetic energies of the relevant shells, and the appropriate f factors are given in Table I. Using Eq. (5), we obtain a value of 0.751 Ry for the valence-band edge, which is now fivefold degenerate. This is fairly close to what would be extrapolated from Fig. 4 if the gap states were ignored. Thus, in going from icosahedral symmetry to the rational approximant with $n/m=5/3$, one has the following scenario: a fivefold-degenerate valence-band edge is split into a quadruplet and a singlet. The singlet corresponds to the edge of the gap states, while the quadruplet is seen as a minor feature in the valence band, at around 0.72 Ry in Fig. 1(a). I have thus confirmed the band-edge-splitting mechanism hypothesized in the pseudo-Jones-zone analysis.

As the order of the rational approximant increases, two important changes occur. First the kinetic-energy splittings between the two pairs of shells in Table I become smaller; these splittings are approximately linear in $|n/m-\tau|$. Secondly, the signs of the splittings alternate with the order of the rational approximant, in the sense that for $n/m=8/5$, the energy of the threefold shell is lower than that of the pseudothreefold, for $n/m=13/8$ it is higher, and so on. Thus if one skips alternate rational approximants and takes the sequence

$$n/m=5/3\rightarrow n/m=13/8\rightarrow n/m=34/13\ ,$$

etc., one expects that the width of penetration of the gap states should be approximately proportional to $n/m-\tau$. If one instead considers $n/m=8/5, 21/13$, etc., one finds that the fourfold pseudothreefold states, instead of the singlet states, are the gap states. These do not penetrate as far into the gap, and essentially merge with the valence band edge.

VI. CONCLUSIONS AND APPLICATION TO AlCuLi

My main conclusions are that band-gap formation in icosahedral quasicrystals can be strongly enhanced without a high-degeneracy shell of **Q** vectors, and that the size of the gap increases as icosahedral symmetry is approached. These effects are smaller if the potential is too weak to form a gap; in this case the electronic structure in the vicinity of the quasigap is fairly well converged already for low-order rational approximant structures. Furthermore, in the cases with gaps, the band-gap reduction due to the breaking of icosahedral symmetry is due to gap states that arise from the splitting of the valence-band edge. So far no quasicrystals with band gaps have been observed. However, our results may be relevant to the AlCuLi system. For appropriate electron concentrations, both its stable icosahedral quasicrystal form and its rational approximant of the Frank-Kasper type have a Fermi-level DOS reduced by a factor of nearly 1/3 relative to the free-electron value.[1-4] The approximant corresponds to our $n/m=5/3$ model, although, as mentioned above, it is known as the "1/1 approximant" to the quasicrystal. One of the several possible shells of **Q** vectors with $Q\approx 2k_f$ comprises an icosahedron and has the indices (311111) in the scheme of Elser.[15] This shell may be responsible for the quasigap effects mentioned above. Previous analysis[8,11] has focused on the (222100) shell because it gives the most intense x-ray scattering. However, the x-ray scattering is dominated by Cu, which, at least in the rational approximant, is irrelevant for the formation of the quasigap.[7] Thus the (311111) shell may be as important as the (222100) shell in creating the potential responsible for the quasigap. In AlCuLi, very small differences in electronic properties between the quasicrystal and the rational approximant are usually observed,[1,3] consistent with my result that in the quasigap case [cf. Fig. 1(b)] the electronic structure is practically converged (as a function of the order of the rational approximant) for the $n/m=5/3$ case. Placing the AlCuLi quasicrystal and rational approximant under high pressure may convert the quasigaps into actual band gaps. This contention is based on *ab initio* band calculations that I have performed for Li. These calculations give the pressure dependence of the band gap at the face of the first Brillouin zone, which is roughly a measure of the strength of the pseudopotential. The results indicate that the Li pseudopotential becomes stronger under pressure, *even when scaled by the Fermi energy.* According to the present results, this could open up a band gap, which should appear in the quasicrystal before the rational approximant.

ACKNOWLEDGMENTS

I am grateful to Jim Sethna for help in techniques for diagonalizing large matrices. The numerical calculations were performed at the Production Supercomputer Facility of the Center for Theory and Simulation at Cornell University, under NSF Grant No. DMR-8614232. This work was supported by the United States Department of Energy under Grant No. DE-FG02-84ER45130.

[1] J. L. Wanger, B. D. Biggs, K. M. Wong, and S. J. Poon, Phys. Rev. B **38**, 7436 (1988).

[2] K. Kimura, H. Iwahashi, T. Hashimoto, S. Takeuchi, U. Mizutani, S. Ohashi, and G. Itoh, J. Phys. Soc. Jpn. **58**, 2472 (1989).

[3] U. Mizutani, A. Kamiya, T. Matsuda, K. Kishi, and S. Takeuchi, J. Phys. Condens. Matter **3**, 3711 (1991).

[4] K. Wang, P. Garoche, and Y. Calvayrac, in *Proceedings of the Codest ILL Workshop on Quasicrystalline Materials,* edited by C. Janot and J. M. Dubois (World Scientific, Singapore, 1988), p. 372.

[5] P. A. Bruhwiler, J. L. Wagner, B. D. Biggs, Y. Shen, K. M. Wong, S. E. Schnatterly, and S. J. Poon, Phys. Rev. B **37**, 6529 (1988).

[6] H. Matsubara, S. Ogawa, T. Kinoshita, K. Kishi, S. Takeuchi, K. Kimura, and S. Suga, Jpn. J. Appl. Phys. **30**, L389 (1991).

[7] T. Fujiwara and J. Yokokawa, Phys. Rev. Lett. **66**, 333 (1991).

[8] J. Friedel and F. Denoyer, C. R. Acad. Sci. (Paris) **305**, 171

(1987).
[9]J. Friedel, Helv. Phys. Acta **61**, 538 (1988).
[10]A. P. Smith and N. W. Ashcroft, Phys. Rev. Lett. **59**, 1365 (1987).
[11]V. G. Vaks, V. V. Kamyshenko, and G. D. Samolyuk, Phys. Lett. A **132**, 131 (1988).
[12]N. W. Ashcroft, Phys. Rev. B **19**, 4906 (1979).
[13]M. L. Cohen and V. Heine, in *Solid State Physics: Advances in Research and Applications,* edited by H. Ehrenreich, F. Seitz, and D. Turnbull (Academic, New York, 1970), Vol. 24, p. 37.
[14]See D. A. Papaconstantopoulos, *Handbook of the Band Structure of Elemental Solids* (Plenum, New York, 1986).
[15]V. Elser, Phys. Rev. B **32**, 4892 (1985).